CHAPTER III

CHARACTERIZATION TECHNIQUES

Our films were characterized using various techniques such as X-ray diffractometry, field emission scanning electron microscopy, atomic force microscopy and optical spectroscopy, respectively. X-ray diffraction technique were used to study crystal structure of the films including the contamination substances which could be found in the films during the film processing. The compositions of the films were obtained using a wavelength dispersive X-ray spectrometer (WDX) equipped with an electron probe microscopic spectrometer (EPMS) and energy dispersive X-ray spectrometer (EDX) equipped with field emission scanning electron microscopy (FSEM: HITASHI model S-4700) . The roughness of our films are determined by atomic force microscopy (AFM). The optical transmittance spectra of the films were measured using UV-VIS-NIR spectrometer. The refractive index and the extinction coefficient before and after gamma irradiation as a function of the gamma dose were extracted from the transmittance spectra using the envelope method [41]. The band gap was also calculated from the transmittance spectra using the Tauc relation [42].

3.1 X-ray diffraction

X-rays is the electromagnetic radiation with energies in the range of 100 eV - 100 keV. X-ray was discovered by Wilhelm Röntgen. X-ray techniques provide important tools for scientists and researchers and use in the field of material characterization. X-ray diffractometers are used for the study of mineral deposits, thin

films and phase transformations. The wavelength of X-rays suitable for measuring the crystal structure is in the range from 0.5 Å to 3 Å that is comparable to the size of atom. In general, the X-ray wavelength value depends on a type of the target used as the anode in a vacuum tube. For example, the X-ray which has a wavelength of 1.54 Å are produced by accelerated electron beam with high voltage collided with the Cu target. When the X-ray incident beam falls onto a crystal, the beam are diffracted. The angle of incidence formed by a ray incident on a surface and a perpendicular to the surface at the point of incident is equal to the reflection angle which is measured from the reflected ray to the surface normal.

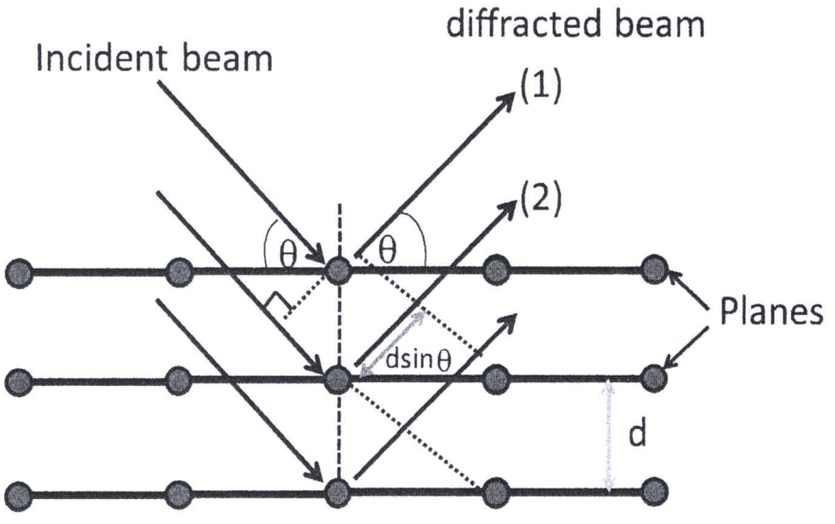

Figure 3.1: X-ray diffraction from crystal structure by Bragg'law.

From Fig. 3.1, when the path difference between path(1) and path(2) equals to an integer number, n times λ, constructive interference will occur

$$2d\sin\theta = n\lambda \tag{3.1}$$

where d is a spacing between successive atomic planes in the crystal; θ is the incident angle between the lattice plane and the incident beam; λ is wavelength of X- ray beam; n is an integer number.

Equation 3.1 is known as Bragg's law. The constructive interference signals can be detected by a detector in form of intensity at varied diffraction angles (2θ). For the same element or material, the intensity of the constructive is the highest at the same diffraction angle. The interplanar spacing of (hkl) planes can be defined by d = d_{hkl}, where h, k and l are Miller indicies. The relationship between the Miller indicies, lattice constants (a,b,c) and interplanar spacing for BTO of tetragonal phase and CCTO of the cubic structure can be shown in equation (3.2) and equation (3.3), respectively.

$$\frac{1}{d^2} = \frac{h^2 + k^2}{a^2} + \frac{l^2}{c^2} \tag{3.2}$$

$$\frac{1}{d^2} = \frac{h^2 + k^2 + l^2}{a^2} \tag{3.3}$$

For standard BTO, the lattice constants equal to 0.3994 nm for a and b and 0.4038 nm for c [24], respectively. The lattice constants of standard cubic CCTO are a = b = c = 0.73798 nm [27].

3.2 Wavelength dispersive X-ray spectroscopy

A wavelength dispersive X-ray spectrometry (WDX) was the original microprobe spectroscopy technique developed to measure X-ray intensities and determine chemical compositions of sample. The main point of the electron microprobe is crystals with specific lattice spacing as shown in table 3.1.

X-rays are produced after an accelerated electron beam collides with the sample. All X-ray will emit at the angle (ψ) to enter the WDS spectrometer. X-ray of each element has a distinct wavelength, and by adjusting the angle of the crystal in the spectrometer, it will diffract the wavelength according to Bragg's law from equation 3.1. The diffraction of X-rays are directed into the detector (proprotional counter tube), which has a thin wire at a middle. The reflected X-rays

Table 3.1: Several crystals used in the wavelength dispersive spectrometer.

Crystal	Plane of crystal	lattice spacing
LiF	(200)	2d = 4.027Å
SiO_2	(1011)	2d = 6.686Å
PG (pyrolytic graphite)	(002)	2d = 6.71Å
PET (pentacrythritol)	(002)	2d = 8.742Å
ADP (ammonium dihydrogen phosphate)	(101)	2d = 10.64Å
KAP (potassium hydrogen phthalate)	(1010)	2d = 26Å

to the detector are different by changing the position of crystals relative to the sample. The sample, crystals and detector are lied on a Rowland circle in order to focus X-ray efficiently. The X-rays are absorbed by gas molecules in the proportional counter tube, photoelectrons is emitted in this process. Photoelectrons are accelerated to a wire in order to add ionization. Two general types of detectors are used to seal and flow of gas to the counter. The seal of proportional counters have a thick window that protects leakage of gas in the detector. Another one is the gas flow proportional counter which have thin window. The X-ray intensities of each element of sample are counted in a detector at a specific beam current. the count rates are compared to those of standards containing known values of the elements of sample.

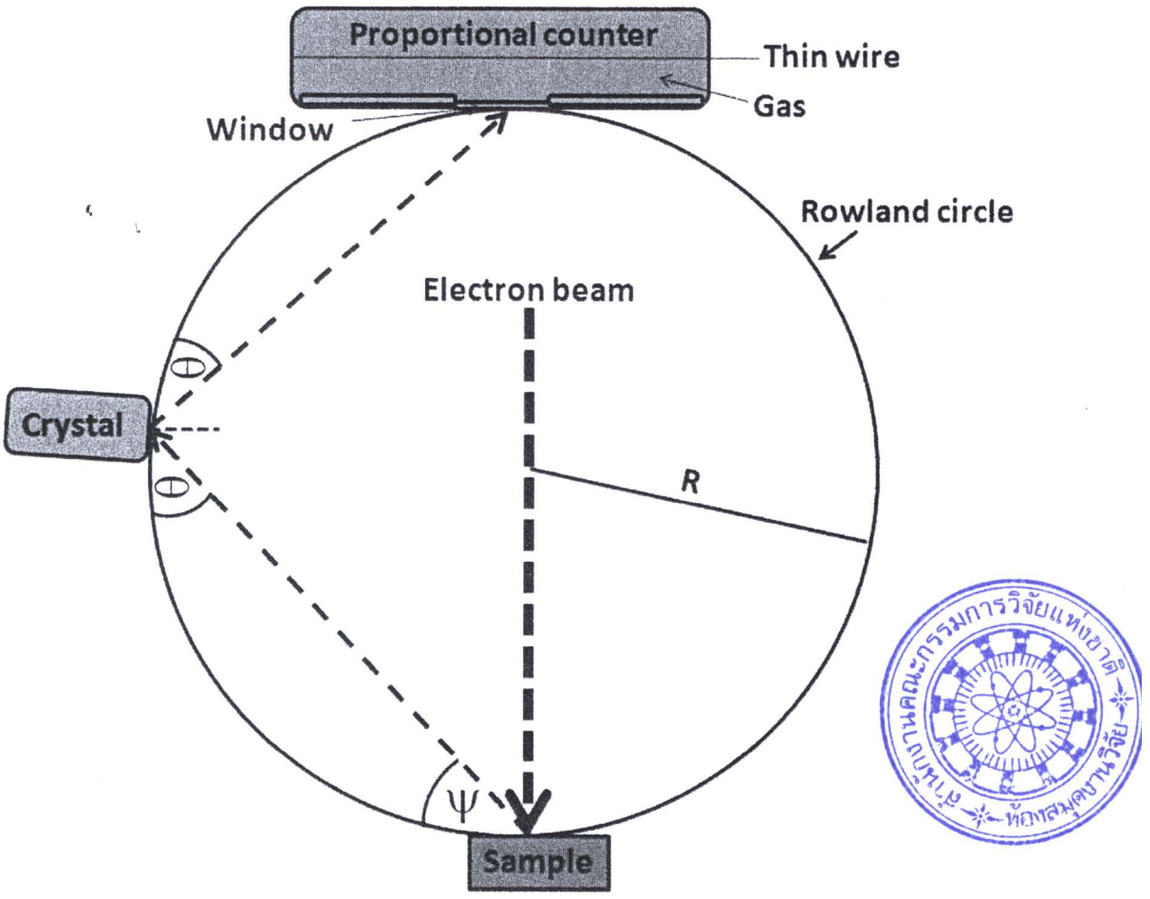

Figure 3.2: Configuration of sample, analytical crystal and detector on the Rowland circle within the WDX spectrometer.

3.3 Energy dispersive X-ray spectroscopy

Energy dispersive X-ray spectroscopy (EDX) is an analytical technique used for the elemental analysis or chemical characterization of a sample. It is one of the variation of X-ray fluorescence spectroscopy which depends on the investigation of a sample through interactions between electromagnetic radiation and the matter. Its characterization ability are exactly in large part to the fundamental principle that each element has a unique atomic structure allowing X-rays that are characteristic of an element's atomic structure to be identified uniquely from one another. To stimulate the emission of characteristic X-rays from a specimen, a high-energy beam of charged particles such as electrons or protons, or a beam of X-rays, is focused into the sample being studied. At rest, an atom within the sample contains ground state electrons in discrete energy levels or electron shells bound to the nucleus. The incident beam may excite an electron in an inner shell, ejecting it from the shell while creating an electron hole where the electron was. An electron from an outer, higher-energy shell then fills the hole, and the difference in energy between the higher-energy shell and the lower energy shell may be released in the form of an X-ray as shown in Fig. 3.3. The number and energy of the X-rays emitted from a specimen can be measured by an energy dispersive spectrometer. As the energy of the X-rays are characteristic of the difference in energy between the two shells, and of the atomic structure of the element from which they were emitted, this allows the elemental composition of the specimen to be measured.

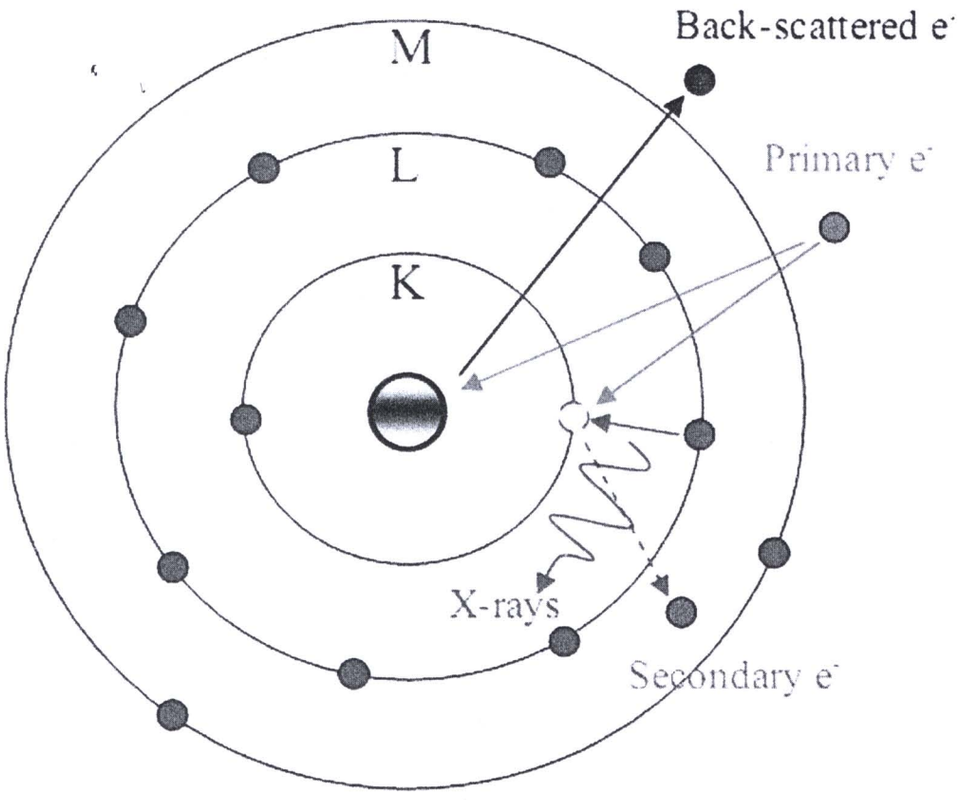

Figure 3.3: Schematic drawings of the x-ray radiation from an atom.

3.4 Atomic force microscopy

Atomic Force Microscopy (AFM) is one of the most useful instruments for characterizing surface morphology of materials. The force most commonly associated with atomic force microscopy is an interatomic force called the van der Waals force. AFM process did not use lens and the sample preparation is not difficult. The key of AFM is a cantilever arm. A laser beam is directed toward the back of the cantilever. A sharp tip is on the free end of the cantilever which has a spring constant of the order of 1 N/m. A laser beam reflects off the end of the cantilever onto a photodetector.

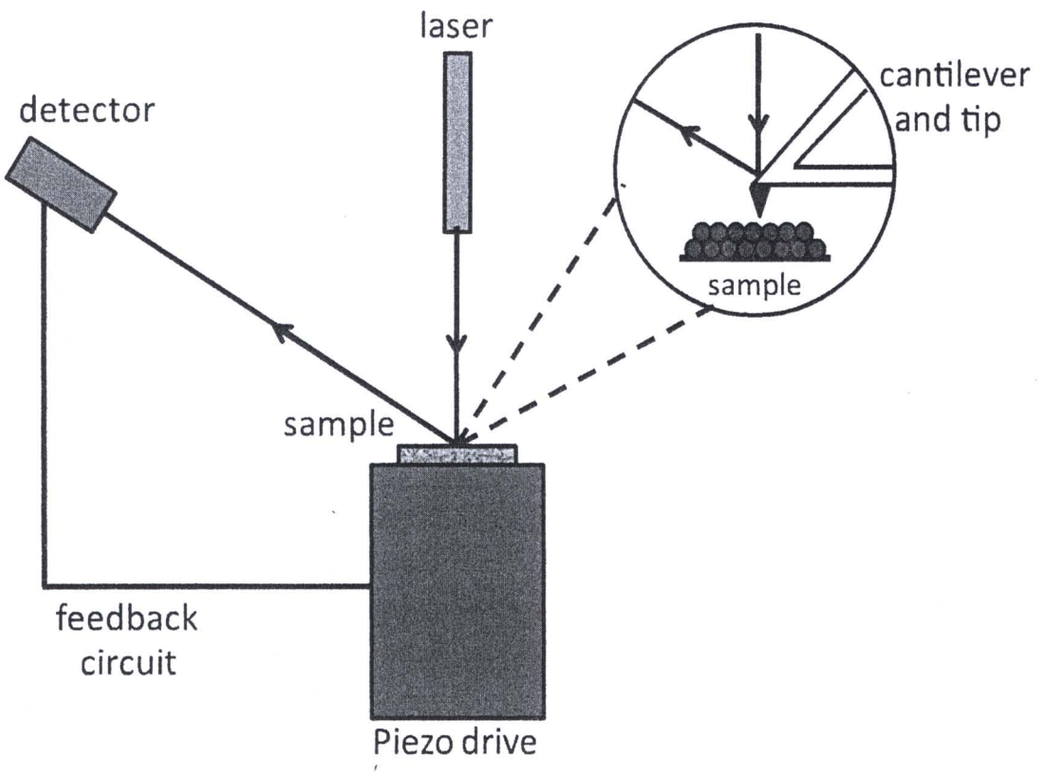

Figure 3.4: Schematic of the atomic force microscope.

The photodetector senses the deflection of cantilever beam as the atom of the sharp tip interacts with the surface atom of the sample. The process of AFM is shown in Fig. 3.4. A piezoelectric scanner pulls the probe across the surface to be imaged. The changes in surface topography cause the probe tip to move up or down, the photodetector senses the motion, and the microscope's computer translates the deflection to surface information in three-dimension. Sample must be cleaned before taking measurements. The interaction force between the cantilever and the sample is replusive when the tip is too close to the sample surface as shown in Fig. 3.5.

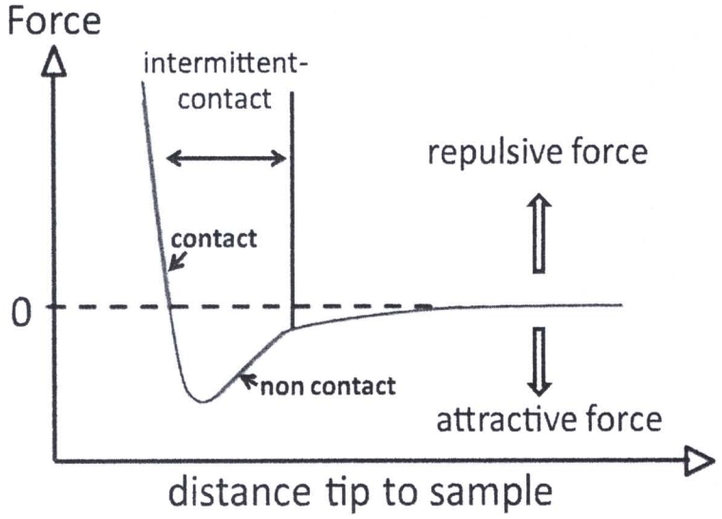

Figure 3.5: AFM operating force regions.

Repulsive forces increase as the probe begins to contact the surface. The repulsive forces in the AFM tend to cause the cantilever to bend up. In the non contact regime, the cantilever is held on the order of 10-100 Å at the resolution in x-y plane range from 0.1 to 1.0 nm and the z direction is 0.01 nm known as atomic resolution. The atomic force between the cantilever and the sample is attractive when the the tip is too far to the sample surface. Attractive forces near the surface are caused by a nanoscopic layer of contamination that is present on all surfaces in surrounding air. The amount of contamination depends on the environment in which the microscope is being operated. In the intermittent contact regime, the vibrating cantilever tip is brought closer to the sample so that the tip just taps the sample. Changing tips and techniques can also provide difference information. The intermittent contact mode or tapping mode was used in this thesis. In tapping mode AFM the cantilever is oscillating close to its resonance frequency. The tips mainly used for tapping mode are silicon probes.

3.5 Optical transmission

The optical measurement method is mostly considered to be quick, easy and nondestructive. The principle is based on the interference of two beams of light which the optical path difference is related to the films thickness [43, 44]. The derivation of the thickness of thin film from the transmission spectra was shown in section 2.5. The films need to be grown on a transparent substrate such as glass slices [41] and quartz [45] in order to detect the transmitted beam.

The schematic diagram of the optical system is shown in Fig. 3.6. There are two radiation sources, a deuterium lamp (DL) and halogen lamp (HL) to cover the whole wavelength range of the spectrometer. The operation of optical system can be described as the following.

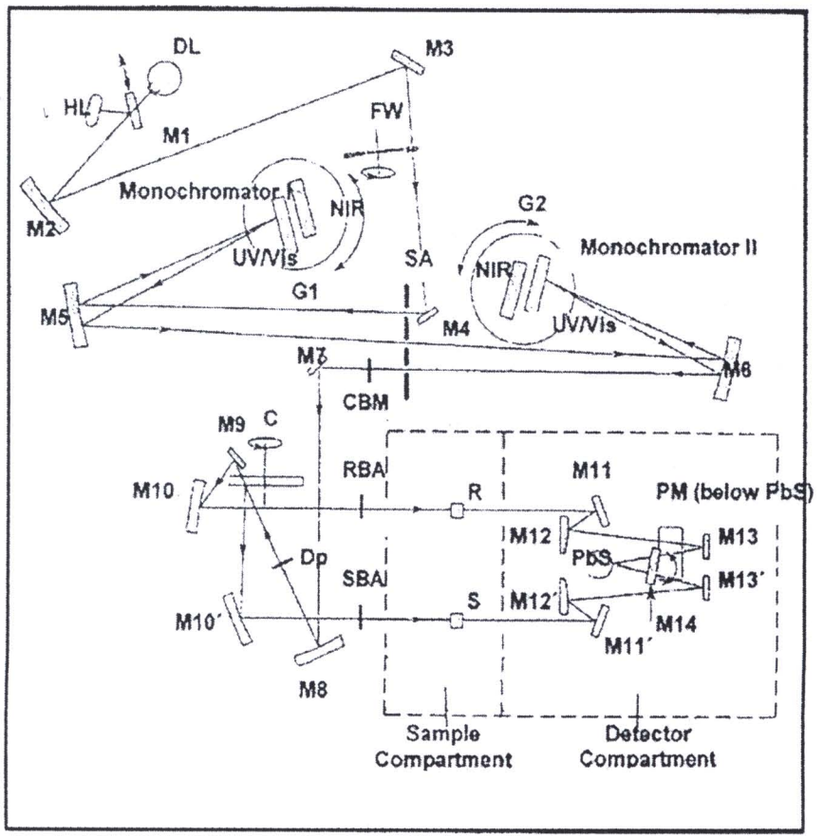

Figure 3.6: Schematic of optical system.

For the operation in the near infrared (NIR) and visible (VIS) ranges, the radiation from halogen lamp is reflected from mirror M1 to M2. At the same time, it blocks the radiation from deuterium lamp. For operation in the ultraviolet (UV) range, mirror M1 is raised to permit radiation from the deuterium lamp to mirror M2. Radiation from the respective source lamp is reflected from mirror M2 to mirror M3 through an optical filter wheel assembly (FW) to mirror M4. The radiation is reflected through the entrance slit of monochromator I, which collimates the radiation. The collimated radiation is reflected at the grating G1. Depending on the current wavelength range, the collimated radiation beam strikes either the UV/VIS grating or the NIR grating.

The radiation is dispersed at the grating to produce a spectrum. The rotational position of the grating effectively selects a segment of spectrum, reflecting this segment to mirror M5 and then through the exit slit serving as the entrance slit of Monochromator II. The radiation is reflected via mirror M6 to the grating on grating table G2 and then back via mirror M6 through the exit slit to mirror M7. The rotational position of grating table G2 is synchronized to that of G1. From mirror M7 the radiation beam is reflected via mirror M8 to the chopper assembly (C).

The chopper separates the radiation into two beams. As the chopper rotates, especially, a mirror segment and a window segment, are brought alternately into the radiation beam. When a window segment enters the beam, radiation passes through to mirror M9 and is then reflected via mirror M10 to create the reference beam (R). On the other hand, when a mirror segment enters, the beam of radiation is reflected via mirror M1$\acute{0}$ to from the sample beams (S).

In the sample compartment, a clean substrate is used as a reference and the sample is thin film coated on one side of substrate. The radiation beam passing alternatively through the sample and a reference are reflected by M11, M12, M13 and M1$\acute{1}$, M1$\acute{2}$, M1$\acute{3}$ of the optics in the detector assembly. Mirror M14 is rotated to select the appropriate detector. A photomultiplier (PM) is used in the UV/VIS range while a lead sulfide (PbS) detector is used in the NIR range.

The optical transmission of the films were measured in the percentage ratio of the intensity of the beam passing through the sample to the beam passing through the blank substrate (I_0) as shown in Fig. 3.7. The incoming beam is incident normally on the surface of the sample and the reference substrate. The detectors measured the intensity of transmitted beam (I_t and I_0), and the percentage of optical transmission can be expressed as

$$T(\%) = \frac{I_t}{I_0} \times 100 \tag{3.4}$$

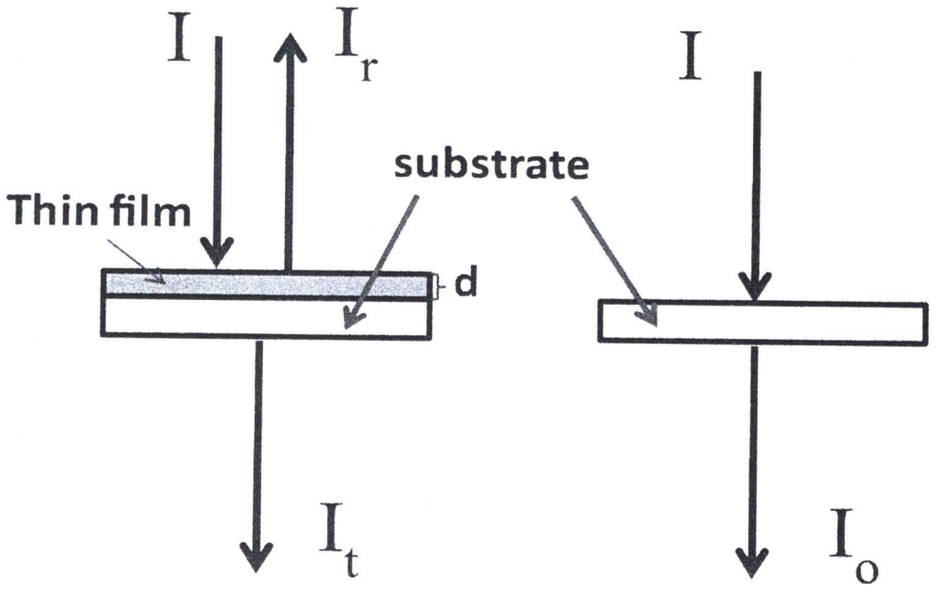

Figure 3.7: Schematic drawing of optical transmission measurement.

The absorbtion coefficient can be calculated directly from the transmission of the films. The transmittance (T) and the reflectance (R) can be expressed in terms of the intensity of transmitted wave I_0 from blank substrate, intensity of transmitted wave I_t from thin film and intensity of reflected wave I_r as the followings;

$$T = \frac{I_t}{I_0} = \frac{(1-R)^2 e^{-\alpha d}}{1 + R^2 e^{-2\alpha d}} \tag{3.5}$$

$$R = \frac{I_r}{I_0} = \frac{(n-1)^2 + k^2}{(n+1)^2 + k^2} \tag{3.6}$$

where α is the absorption coefficient; d is the thickness of the film; n is refractive index and k is extinction coefficient.

If the film has a large thickness (d), then

$$R^2 e^{-2\alpha d} \ll 1$$

and equation 3.6 can be reduced to

$$T = (1-R)^2 e^{-\alpha d} \tag{3.7}$$

In general, the changing of photon energy of incident wave affects the reflection (R) slightly. Then, the term $(1\text{-}R)^2$ can be approximated to a constant. From equation 3.7, the absorbtion coefficient is

$$\alpha = \frac{1}{d} In(\frac{I_0}{I_t}) + C \tag{3.8}$$

where d is the thickness of the film and C is a constant.

3.5.1 Complex refractive index (n and k) and absorption coefficient

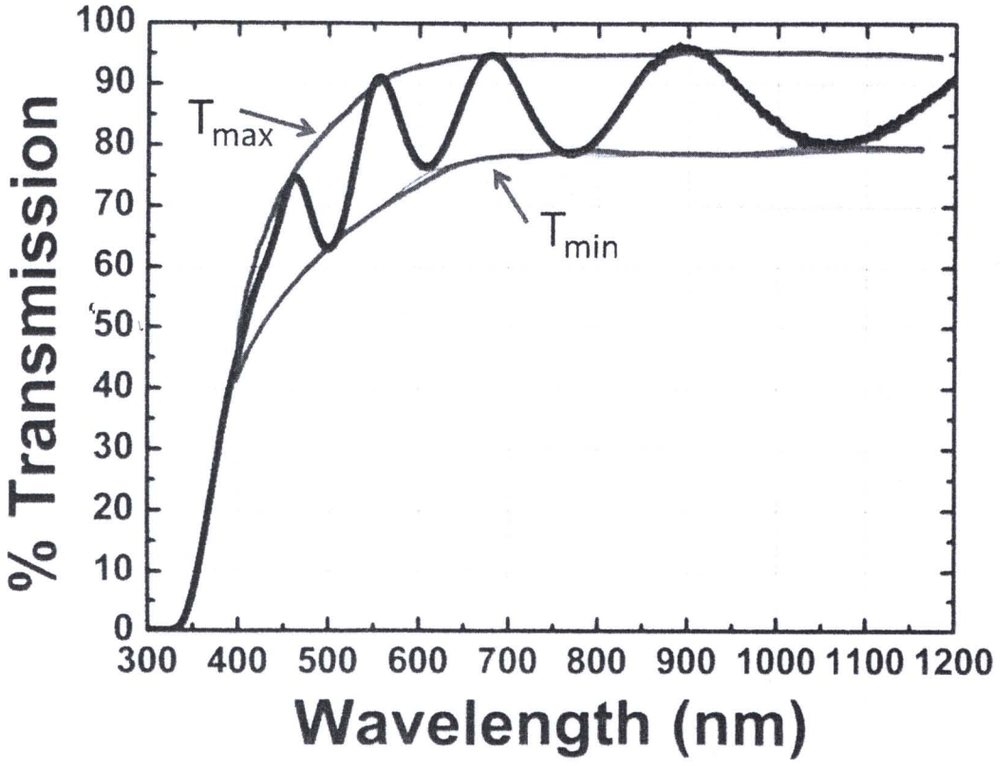

Figure 3.8: Schematic drawing envelope of optical transmission measurement.

When the film has a uniform thickness, the oscillation of transmission spectra can be clearly observed as shown in Figure 3.8. The refractive index can be obtained using an envelope method [41];

$$n(\lambda) = [N + (N^2 - n_s^2)^{1/2}]^{1/2} \tag{3.9}$$

where

$$N = (\frac{n_s^2 + 1}{2}) + 2n_s^2(\frac{T_{\max} - T_{\min}}{T_{\max} T_{\min}})$$

n_s is the refractive index of the substrate, $T_{\max}$ and $T_{\min}$ are the maximum and

minimum transmittances see in Fig. 3.8. The extinction coefficient can be obtained from

$$k = \frac{\alpha\lambda}{4\pi} \tag{3.10}$$

where α is the absorption coefficient;

$$\alpha = \frac{1}{d} \ln \frac{(n-1)(n_s-n)[1+(\frac{T_{max}}{T_{min}})^{\frac{1}{2}}]}{(n+1)(n_s+n)[1-(\frac{T_{max}}{T_{min}})^{\frac{1}{2}}]}$$

d is the film thickness.

3.5.2 Band gap energy

The band gap was also calculated from the transmittance spectra using the Tauc relation [42]. From the transmittance spectra, the energy for the direct gap could be calculated by using the equation

$$(\alpha h\nu)^2 = B(h\nu - E_g) \tag{3.11}$$

where α is the absorption coefficient calculated from equation 3.8, hν is the photon energy, E_g is the energy gap as shown in Fig. 3.9 and B is a constant. By plotting $(\alpha h\nu)^2$ versus hν, the energy band gap can be obtained from the intercept of graph for direct allowed transition. The photon energy at the point where $(\alpha h\nu)^2 = 0$ is the energy gap of which value is determined by the extrapolation method. The extrapolation of the linear segment of the spectrum or curve towards the x-axis gives the value of energy gap.

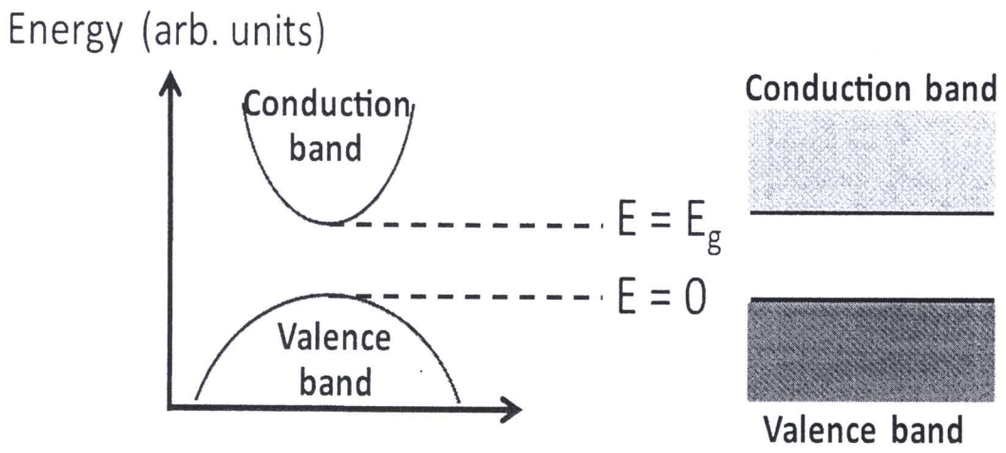

Figure 3.9: Schematic of band diagram.

Fig. 3.10 shows the band diagram of (a) n-type semiconductor and (b) p-type semiconductor, respectively. When an impurity atom with more valence electrons substitutes the atom in lattice inducing electron carriers as major carriers ($n \gg p$), this material is so called n-type semiconductor. In Fig. 3.10(a), n-type semiconductor yields electrons to the conduction band. While the p-type semiconductor occurs when an impurity atom with less valence electrons substitutes the atom in lattice. The state corresponding to the missing electrons is therefore the holes. The number of holes similar to the number of impurities is created. Consequently, the impurities called acceptors, can create holes in the valence band. In Fig. 3.10(b), the impurity levels can be presented at an acceptor level above the valence band edge.

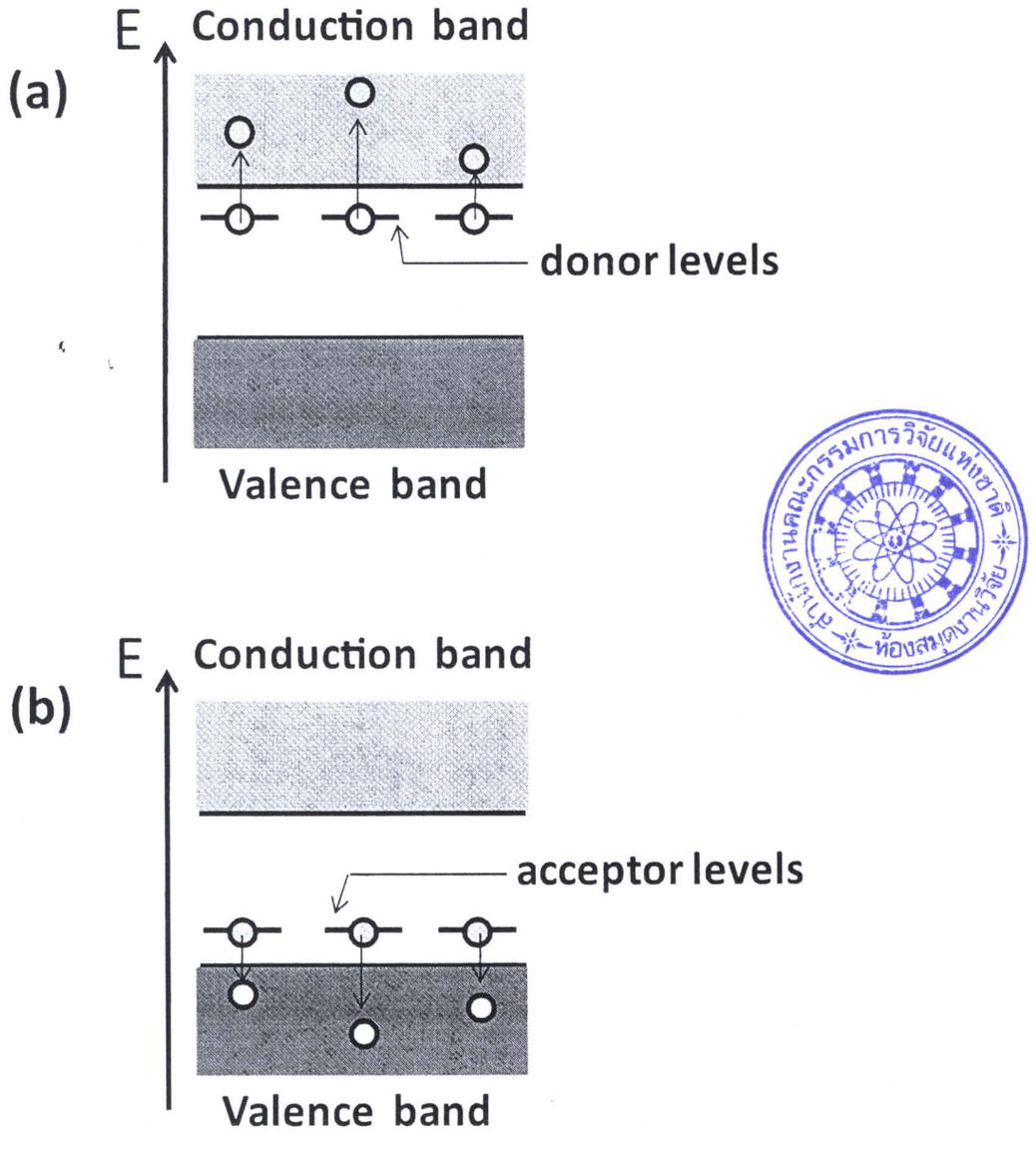

Figure 3.10: The band diagram of (a) n-type semiconductor (b) p-type semiconductor.